

# Conducting Polymer-Based Biocomposites Using Deoxyribonucleic Acid (DNA) as Counterion

Serpil Tekoglu, Dominik Wielend, Markus Clark Scharber, Niyazi Serdar Sariciftci, and Cigdem Yumusak\*

In this work, the preparation of conducting polymer-based composites using a biological anionic polymer based on salmon deoxyribonucleic acid (DNA) is presented. The most commonly used polymers poly(3,4-ethylenedioxythiophene) (PEDOT), as well as polypyrrole, are polymerized in the presence of DNA. Since conjugated polymers are in the polycationic state in their electrically conducting form, the role of the counterion is now fulfilled by the low cost biomolecule DNA as an alternative material, which is also a polyanion thanks to its phosphate chain. The resulting synthesized material is a conducting polymer–DNA biocomposite. Such materials are highly attractive for the rising field of bioelectronics and biosensors, especially in organic electrochemical transistors (OECTs) and ion pumps. OECTs made of these conducting polymer biocomposites are fabricated and their electrochemical device operation is compared to the most widely used PEDOT:polystyrenesulfonate.

introducing functional devices with dual electronic–ionic capability as well as other selective side groups are possible.<sup>[24,26]</sup>

Polyaniline and polypyrrole among the oldest conducting polymers are dating back as early as 1830.<sup>[27–31]</sup> Polypyrrole (earlier called as pyrrole black) (Figure 1a) is relatively easy to synthesize and has been already utilized for battery and supercapacitor applications.<sup>[22]</sup> However, such polymers in the class of the first generation conductive polymers are in general insoluble and, therefore, not processable. Finally, the development of a new polythiophene derivative poly(3,4-ethylenedioxythiophene) (PEDOT)<sup>[32]</sup> has significantly changed the game.<sup>[33,34]</sup> In PEDOT, the 3,4 positions are blocked enforcing the regioregularity of polymerization

## 1. Introduction

Bioelectronics is a highly emerging field using semiconductor devices in both directions to stimulate the bioactivity in living systems as well as detecting and signaling bioactivity in the presence of biomolecules.<sup>[1–12]</sup> Most of the biosystems work in aqueous media utilizing electrochemical signal transduction and ionic channels; however, the silicon-based electronic devices are in their crystalline form using electronic conduction only. Interfacing biology and electronics, thus need to have an important requirement for the devices and materials: a mixed electronic/ionic conductivity.<sup>[13–29]</sup> One way to achieve this requirement is to use conjugated organic semiconductors and conductive polymers.<sup>[21–26]</sup> These materials consist of conjugated,  $sp^2$ -hybridized electronics systems with tunable physical and chemical properties by chemical synthesis.<sup>[26]</sup> As such

(see Figure 1b). Since the conducting phase of the conjugated polymers is in their polycationic form, a counterion-induced solubility has been introduced by incorporating polystyrenesulfonate (PSS) as the polyanion. Thus, PEDOT:PSS composite, which is combined with two polyelectrolytes (polyanionic and polycationic salts) is soluble, dispersible as well as processable. Eventually, the water soluble/processable polyelectrolyte system PEDOT:PSS became a flagship material for all organic electrochemical transistor applications.<sup>[35–42]</sup>

Indeed, the development of organic electrochemical transistors (OECTs),<sup>[43]</sup> electrolyte-gated organic field effect transistors (EGOFETs),<sup>[44]</sup> organic electrochemical biosensors,<sup>[45]</sup> and many other electron/ion delivery devices<sup>[46,47]</sup> gives rise to a new subfield of organic electronics named as iontronics which is mainly focused on the materials and devices which can utilize the coupling of electrical and ionic signals.

The most well-known iontronic device is likely the OECT, which is capable of simultaneous control of electronic and ionic currents. Since the conductive channel is in direct contact with the electrolyte in this device concept, OECTs can convert (bio)chemical signals into electronic ones, which makes them efficient transducer for chemical and biological sensing applications.<sup>[4,5,10,48]</sup>

The first OECT has been introduced in 1984 by White et al. in which electropolymerized PPy has been used to fabricate p-type accumulation mode devices.<sup>[43]</sup> After this pioneering work, several other organic conjugated polymers such as polyaniline,<sup>[49]</sup> polycarbazole,<sup>[50]</sup> and polythiophene<sup>[51]</sup> based devices have also been demonstrated. There is already a large body of scientific work published in the field of OECT applications,

S. Tekoglu, D. Wielend, M. C. Scharber, N. S. Sariciftci, C. Yumusak  
Linz Institute for Organic Solar Cells (LIOS)  
Physical Chemistry  
Johannes Kepler University Linz  
Altenbergerstraße 69, 4040 Linz, Austria  
E-mail: cigdem.yumusak@jku.at

 The ORCID identification number(s) for the author(s) of this article can be found under <https://doi.org/10.1002/admt.201900699>.

© 2019 The Authors. Published by WILEY-VCH Verlag GmbH & Co. KGaA, Weinheim. This is an open access article under the terms of the Creative Commons Attribution License, which permits use, distribution and reproduction in any medium, provided the original work is properly cited.

DOI: 10.1002/admt.201900699

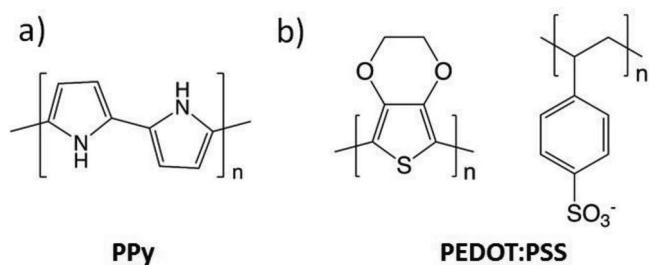


**Figure 1.** Chemical formula of a) polypyrrole (PPy) and b) poly(3,4-ethylenedioxythiophene):polystyrenesulfonate (PEDOT:PSS).

which goes beyond the scope of this paper but studied properly in other articles in many journals.

On the other hand, the biocompatibility of PEDOT:PSS is still under debate in terms of long-term biocompatibility<sup>[17,52,53]</sup> even though an United States Food and Drug Administration approval for specific medical products has been issued.<sup>[54]</sup> Today significant work is still being dedicated toward chemical modifications and further improvements of PEDOT:PSS<sup>[55,56]</sup> and meanwhile substantial effort is devoted to develop alternative conjugated polymer structures.<sup>[57–63]</sup> Therefore, the search of new conducting polymer biocomposites is clearly essential to the field of bioelectronics.

Biofunctionalization of conducting polymers has been proposed to improve their biocompatibility and functionality in specific biomedical applications where they interface with living cells.<sup>[64]</sup> Peng et al. reviewed the immobilization of DNA sample fragments on the films of conducting polymers including PEDOT and PPy film for DNA sensing.<sup>[65]</sup> Recently, PEDOT has been incorporated with the biomolecule dopants, e.g., DNA, hyaluronic acid, dextran sulfonate, heparin, pectin, guar gum to improve the biocompatibility.<sup>[66]</sup> Among those, PEDOT:DNA has the main advantage of the high ionic conductivity in respect to PEDOT:PSS.<sup>[67]</sup> However, the thin film morphology of PEDOT:DNA restricted its performance as a semiconductor material for transistor applications.<sup>[68]</sup>

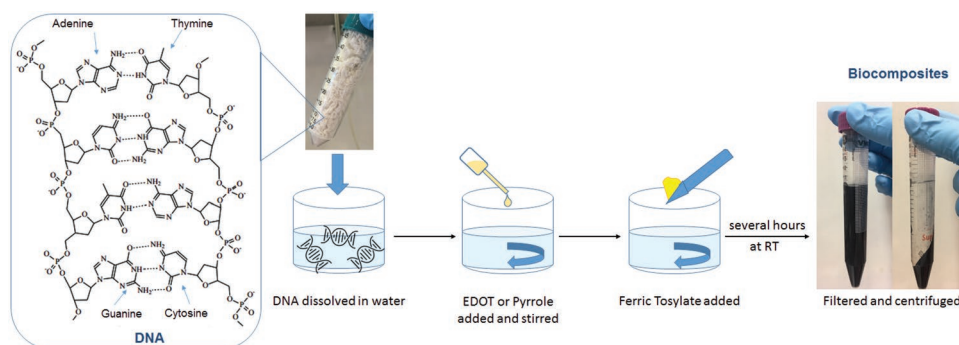
Also the use of polypyrrole biocomposites can be highly interesting bringing back this most famous conducting polymer PPy back into the field of bioelectronics. To the best of our knowledge, there is no application of DNA templated conductive polymer synthesis for using in OECTs.

In this study, we synthesized PEDOT:DNA and polypyrrole:DNA (PPy:DNA) biocomposites to test as conducting polymers in OECTs. The synthesis was performed in aqueous dispersions of the compounds by oxidative chemical polymerization. DNA was engaged as a stabilizer and counterion dopant during the polymerization process of the monomer units. Different additives (surfactants and cross-linkers) were added into the dispersed solution of the biocomposites for appropriate thin film-formation. We successfully deposited the thin layers of conductive polymers from aqueous solutions by using drop-casting and spin-coating methods. Subsequently, we investigated the electrical, optical, and morphological properties of the thin films. The materials were characterized by Raman spectroscopy, atomic force microscopy (AFM), scanning electron microscopy (SEM), and optical absorption techniques. The electrical sheet resistance of the films was determined by using the four-point probe method. Finally, we fabricated and characterized the performance of these materials in OECTs to determine the functionality as compared to the benchmark of PEDOT:PSS devices fabricated under identical conditions.

## 2. Results and Discussion

### 2.1. Synthesis of the Conductive Biocomposites

In order to prepare DNA-doped PEDOT and PPy, we followed the template synthesis method as previously described in the literature.<sup>[67]</sup> The illustrative representation of oxidative chemical polymerization steps is shown in **Figure 2a**. Salmon-based DNA from Prof. Ogata's group in Hokkaido, Japan was received (courtesy of James Grote)<sup>[69–73]</sup> and dissolved in 18 MΩ water and stirred overnight to have a transparent solution with 0.75% solid content. After adding 3,4-ethylenedioxythiophene (EDOT) or distilled pyrrole with the weight composition of 1:0.8 DNA to monomer units, the mixture was stirred for 1 h to obtain a clear solution. Iron(III) p-toluene sulfonate, namely, ferric tosylate (2.5 molar equivalent to monomer) was used as the oxidative reagent. The polymerization of PEDOT:DNA was carried out at room temperature for 48 h or 60 °C for 16 h. The synthesis of PPy:DNA was achieved at 20 °C within 20–30 min. After the polymerization was completed, the product was filtered with water and centrifuged at a speed rate of 5500 rpm for 3 min



of 160 mg/10 mL water was stored in the fridge at +4°C for 1-2 months without degradation.

**Figure 2.** General chemical formula of DNA together with illustrative representation of oxidative chemical polymerization.

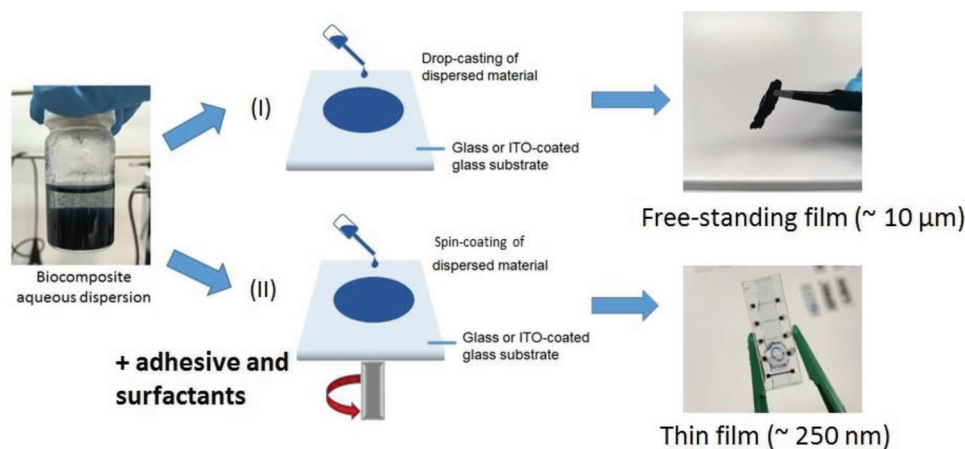


**Figure 3.** Pictorial representation for the film formation of conducting polymer biocomposites. Films were deposited on glass or ITO-coated glass by drop-casting (I) or spin-coating (II) methods. Films were dried at 140 °C for 1 h and subsequently used for analysis. For the process II, the mixture containing 94.5% v/v dispersed solutions, 5% v/v glycerol, and 0.5% v/v DBSA. Afterward 1% v/v GOPS was added into the prepared mixture.

several times. Then, the dispersed solution was sonicated for 4 h and dialyzed for 24 h. The final product with the concentration of 160 mg/10 mL water was stored in the fridge at +4 °C for 1–2 months without degradation.

Raman spectroscopy has been performed to characterize the structural properties of the materials and is discussed in detail in the Supporting Information.

## 2.2. Film Formation and Characterization

PEDOT:PSS films can be easily deposited by spin-coating from a commercially available aqueous dispersion. However, the film processing of newly synthesized biocomposites PEDOT:DNA and PPy:DNA by spin-coating has shown several obstacles resulting in poor film quality. We observed notable microcracks and peel-off problems after the annealing while getting rid of the excess water in the drop-casted films. For PEDOT:PSS-based OECT applications, additives are used to improve the conductivity and as well as mechanical strength to avoid the delamination of the film when it is in contact with aqueous media. 3-glycidoxypropyltrimethoxysilane (GOPS)<sup>[74,75]</sup>

and divinyl sulfone are the commonly used well-known cross-linkers.<sup>[56]</sup> Dodecyl benzene sulfonic acid (DBSA) is widely used as a surfactant for film processing from the commercial suspension.<sup>[15,76]</sup> In 2017, Håkansson et al. improved the adhesion of PEDOT:PSS on a glass substrate with the addition of a small amount of GOPS (0.1% v/v).<sup>[74]</sup> However, GOPS decreases the conductivity of PEDOT:PSS due to the siloxane network. Therefore, secondary dopants, i.e., ethylene glycol, dimethyl sulfoxide, glycerol are employed in the suspension to increase the electrical conductivity of the film.<sup>[76]</sup> According to the optimized volume ratios in ref. [76], we processed the films from the mixture of 94.5% v/v dispersed solutions with the addition of 5% v/v glycerol and 0.5% v/v DBSA. We finally added 1% v/v GOPS to the prepared mixture. We obtained the film formation of biocomposite without further additives via spin-coating and adjusted the film thickness in the range of 250 nm. The film preparation steps and the photo of resulted film formation (drop-casted film  $\approx$ 10  $\mu$ m and spin-cast film  $\approx$ 250 nm) are shown in **Figure 3**.

**Figure 4** represents the transmittance spectra of the conductive films in the visible range of the spectrum. We observed that 260 nm thick PEDOT:DNA thin film shows higher

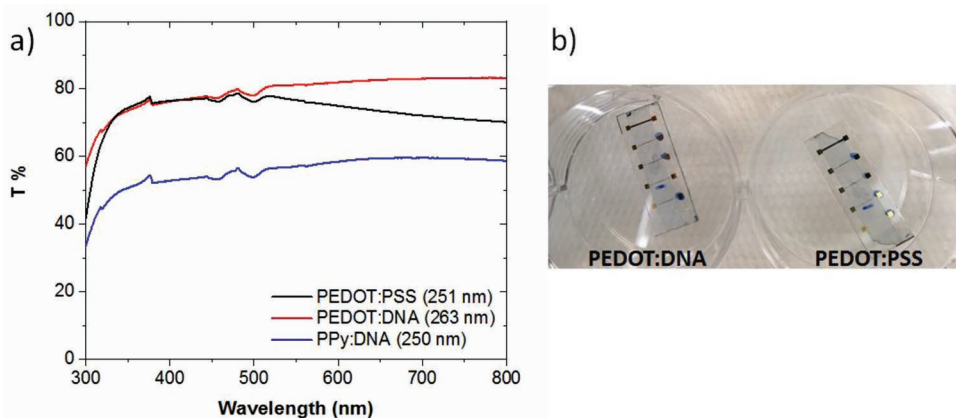


**Figure 4.** a) Transmittance spectra of spin-coated films on glass. b) The photograph of thin layers deposited on the source/drain electrodes for OECTs. All layers were deposited using the same spin-coating parameters as performed for OECTs.

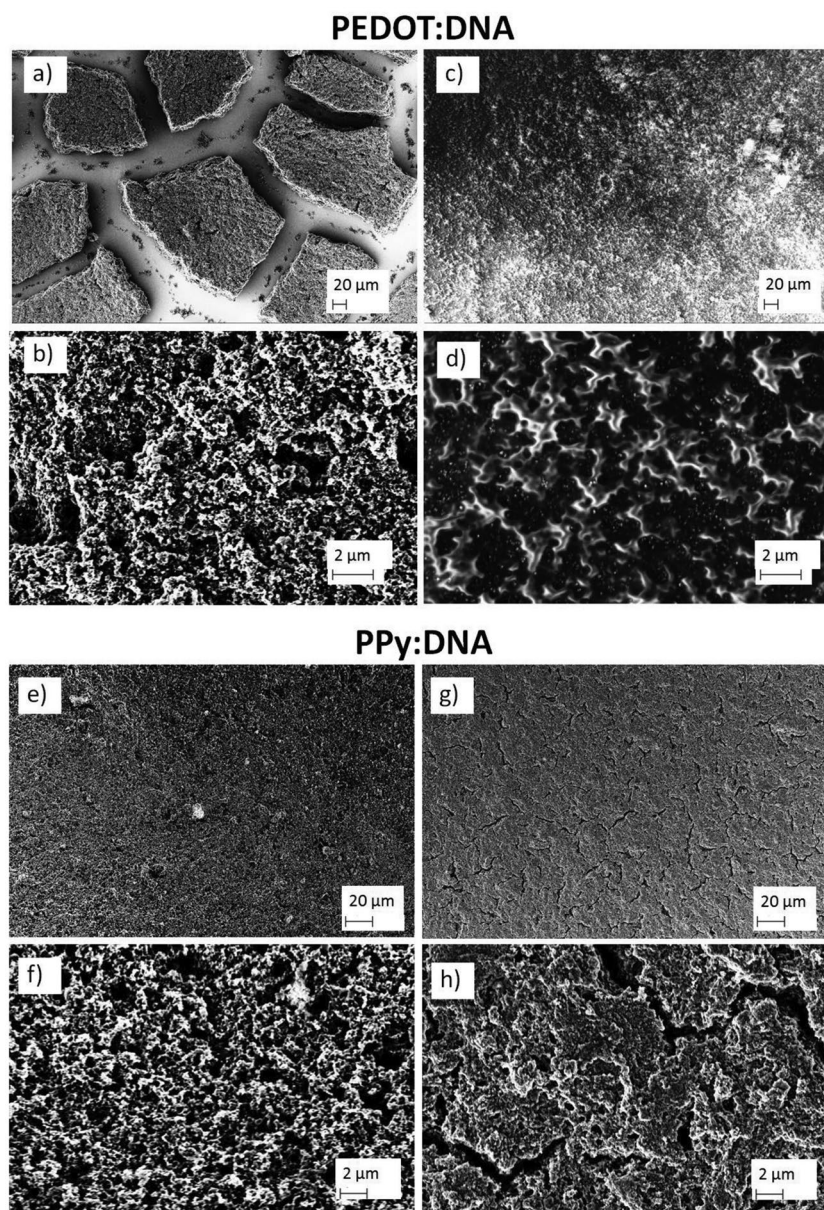


**Figure 5.** Scanning electron microscope (SEM) images of conducting biocomposite films. SEM images of a,b and e,f) the films without additives and c,d and g,h) are the results for the films with the addition of 5% v/v glycerol and 0.5% v/v DBSA. 1% v/v GOPS was added into the final mixture. We observed that the additives bring significant improvement for film formation.

transparency in the IR compared to 250 nm of PEDOT:PSS film and lower transmittance for 250 nm of PPy:DNA film.

The morphology of the films was investigated by SEM and AFM. **Figure 5** exhibits the result of SEM measurements of biocomposite films. The images in **Figure 5a,b** and **Figure 5e,f** indicate the drop-casted films without additives, while **Figure 5c,d** and **Figure 5g,h** show the results for the thin films deposited from the solution of 94.5% v/v dispersed polymers, 5% v/v glycerol, and 0.5% v/v DBSA, with later addition of 1% v/v GOPS into this mixture. Microcracking of the film can be seen on the SEM image (scale bar: 20  $\mu\text{m}$ ) of PEDOT:DNA in **Figure 5a**. After introducing the additives, the microcrack

plane is withdrawn (**Figure 5c**). **Figure 5b** of PEDOT:DNA (scale bar: 2  $\mu\text{m}$ ) shows the uniform film with fiber-like aggregates of template system.<sup>[67]</sup> **Figure 5d** exhibits the changes in the uniform film resulting in coalesced aggregates which confirm the effect of additives in lower magnification. The noticeable morphological change with additives can be attributed to the increase in the conductivity.

The SEM images (scale bar: 20  $\mu\text{m}$ ) of PPy:DNA in **Figure 5e,g** indicate that the additives do not play an essential role for the improvement of the film formation. However, the drop-cast films were delaminated from the substrate, as seen in **Figure 3** (free-standing PPy:DNA film). Therefore, additives were engaged to adhere the film to the glass substrate for device application. **Figure 5f** (scale bar: 2  $\mu\text{m}$ ) presents the uniform film with aggregates of PPy:DNA composite. However, the morphological effect of additives can be observed in **Figure 5h** (scale bar: 2  $\mu\text{m}$ ). The crack formation is noticed at lower magnification while aggregates tend to merge to form islands (uncracked material segments). Revealing the cracking may affect the device performance.

The surface morphology of spin-coated thin films was further analyzed by AFM using tapping mode. The AFM topographic images are shown in **Figure 6**. We used the mixture of 94.5% v/v dispersed solutions, 5% v/v glycerol, 0.5% v/v DBSA, and later the addition of 1% v/v GOPS for all spin-coated films. The root-mean-square (RMS) images are shown in **Figure 6**. We observed continuous film and homogenous distribution of the materials. However, in comparison to PEDOT:PSS film, the topography images of PEDOT:DNA and PPy:DNA represent higher RMS values at the range of 70 nm. PEDOT:PSS film has smooth and homogenous morphology with the low RMS roughness value of  $\approx 4$  nm. This increased roughness of the DNA biocomposites is presumed to originate from the hydrogen bonding organization capability of DNA, giving rise to larger crystallites as compared to the amorphous counterion PSS.

The electrical sheet resistance of the films was measured by using four-point probe and correlated with the OECT device performance. Comparing to the PEDOT:PSS reference with additives, biocomposites have higher sheet resistance (**Table 1**).

### 2.3. OECT Fabrication and Characterization

The device configuration of the OECT can be seen in **Figure 7a**. **Figure 7b** shows the transfer ( $I_D/V_G$ ) characteristics of

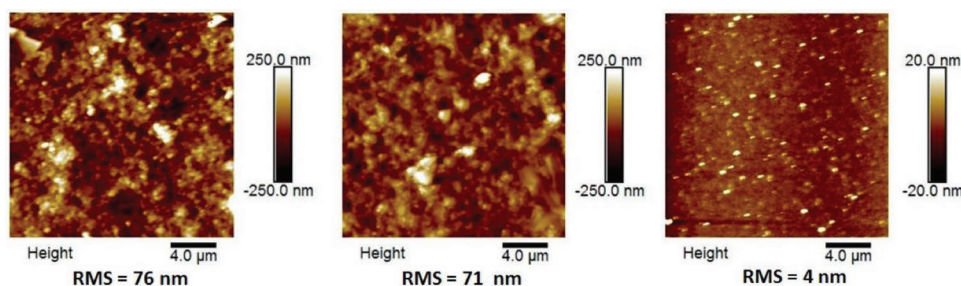


**Figure 6.** AFM images of spin-coated films. All films were deposited from the solution of 94.5% v/v dispersed solutions, 5% v/v glycerol, 0.5% v/v DBSA, and afterward 1% v/v GOPS. The color scale bar in the right represents the height change. The film thicknesses; PEDOT:DNA = 170 nm, PPy:DNA = 250 nm, PEDOT:PSS = 250 nm.

PEDOT:PSS PH1000, which is the most commonly used material in OECT studies and therefore taken here as a benchmark reference. When a positive gate voltage is applied a decrease of the hole density in the PEDOT and therefore the drain current in the channel is observed. Further application of a positive gate voltage shows typical pinch-off saturation behavior seen in Figure 7b. One of the key metrics to define the performance of the OECTs “transconductance” ( $g_m = \partial I_D / \partial V_G$ ), which is defined as the modulation of drain current ( $I_D$ ) in response to small changes in gate bias ( $V_G$ ) was also evaluated. The transconductance of PEDOT:PSS PH1000 peaks at 21.5 mS (at  $V_G = 0$ , source–drain voltage  $V_D = -0.7$  V) however on/off ratio is around 2. Figure 7c shows the OECT output characteristics of PEDOT:PSS PH1000. For an applied negative bias at the drain, while the gate bias is ranging from 0 to 0.4 V, the device shows typical p-channel transistor behavior working in the depletion mode with no saturation indicated in these  $I_D/V_D$  characteristics.

OECT devices output characteristics based on PEDOT:DNA material can be seen in Figure 7e. The device shows a typical p-type transistor behavior with an on/off ratio of  $\approx 300$ . Also a clear indication of saturation is observed at low gate voltages. On the other hand, in comparison to the PEDOT:PSS PH1000 OECT, we note that the drain current has significantly lower values in the DNA composites. Figure 7d shows the transfer curve of PEDOT:DNA OECT. Similarly, it works in depletion mode and has a transconductance value of 160  $\mu$ S.

Figure 7f,g shows the transfer characteristics and the output curves of PPy:DNA, respectively. PPy:DNA-based OECT could reach to low drain current values with an on/off ratio of around

200. Also a clear indication of saturation is observed at all applied gate voltages. However, it shows very low transconductance value of 60  $\mu$ S.

### 3. Conclusion and Outlook

In this work, we introduced conducting polymer biocomposites PEDOT:DNA and PPy:DNA and OECTs thereof. The biocomposite materials have been synthesized in aqueous media by oxidative chemical polymerization while DNA was the counterion (polyanion) for the conducting polymers (polycations). These biocomposites presented herein are in the stage of “proof of concept” of a whole new alternative route for the OECT fabrication, since PEDOT:PSS shall not be the only material investigated in the field.

After introducing different additives to improve the film-formation capability, water dispersion of the final material composition was successfully processed by drop-casting and spin-coating methods. Subsequently, we performed the morphological, spectroscopic, and electrical investigations of the films.

The OECTs have been fabricated and characterized. The results show that the DNA-based conductive polymers can be considered as novel biocomposites materials for all iontronics devices like OECTs and biosensors. In contrast to the most widely used benchmark material PEDOT:PSS we incorporate a biomolecule DNA as counterion in the composite structure. Such composites can be utilized through DNA specific recognition properties. PSS unit in PEDOT:PSS composite do not have biospecific recognition properties. Therefore, we propose such conducting polymer biocomposites with DNA, RNA, peptides, and proteins as an important strategy in future for the bioelectronics.

### 4. Experimental Section

**Materials:** PEDOT:PSS Clevios PH1000 was purchased from Heraeus GmbH and filtered through a polyvinylidene fluoride filter with the pore size of 0.45  $\mu$ m before use. The purified salmon DNA ( $M_w = 8000$  kDa) was provided by Prof. Ogata (courtesy of J. Grote).<sup>[69–73]</sup> All the other reagents (EDOT, pyrrole, ferric tosylate) and additives glycerol, DBSA, and GOPS were purchased from Sigma-Aldrich. All chemicals were used as received, and only pyrrole was distilled prior to use. The chemical synthesis and filtration were achieved in 18 M $\Omega$  ultrapure water. The

**Table 1.** The electrical sheet resistance of the thin films.

Sample	Sheet resistance ( $R_s$ ) <sup>a)</sup> [ $k\Omega$ sq <sup>-1</sup> ]
PEDOT:PSS	0.42
PEDOT:PSS + additives	0.12
PEDOT:DNA	0.55
PEDOT:DNA + additives	0.26
PPy:DNA	0.68
PPy:DNA + additives	0.46

<sup>a)</sup>Sheet resistance was measured at different locations of each sample under the applied current of 10  $\mu$ A.

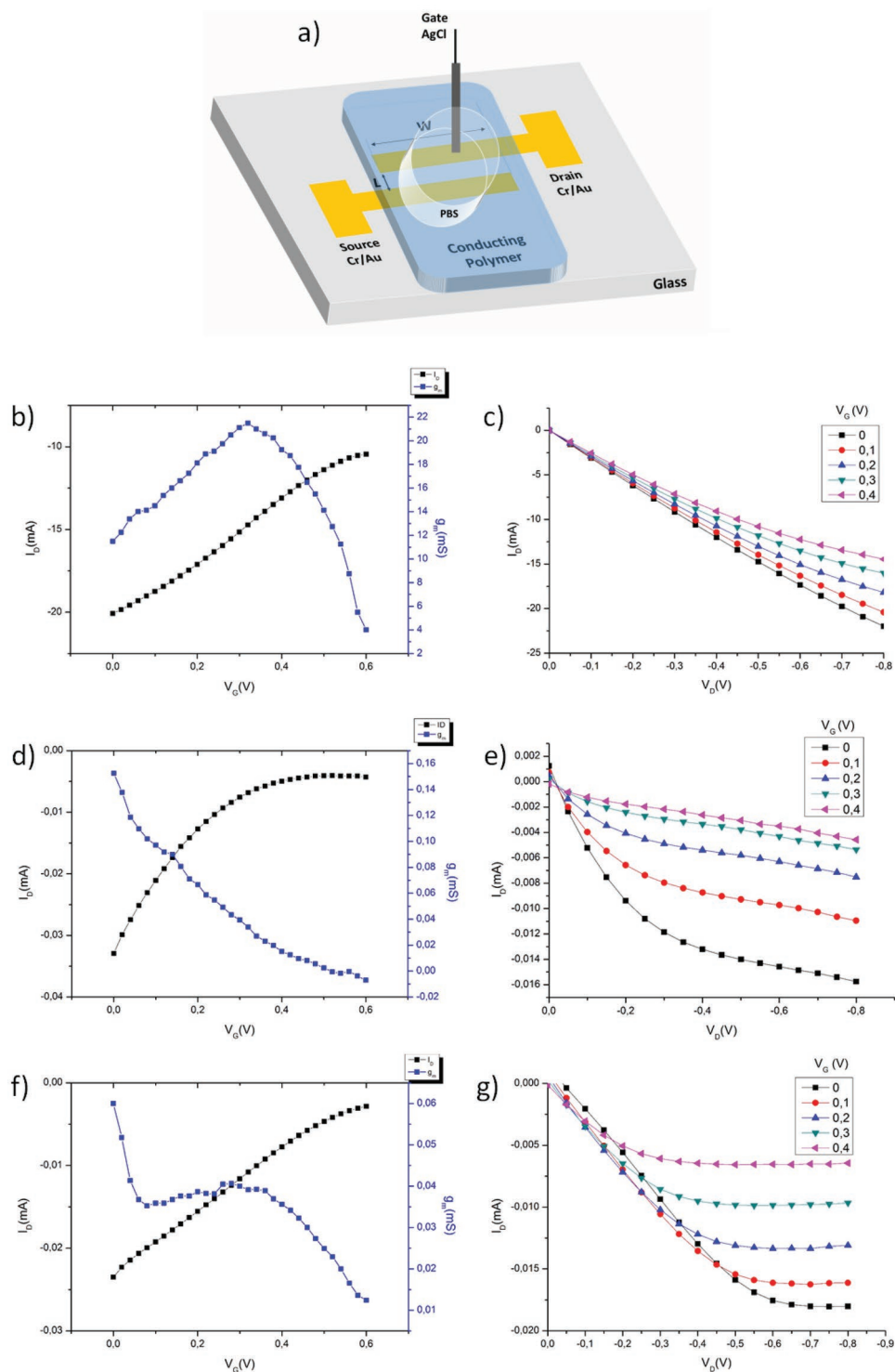


**Figure 7.** a) The schematic illustration of an OEET device. b) Transfer characteristics and the transconductance of PEDOT:PSS reference OEET device ( $g_m = 21.5$  mS for  $V_D = -0.7$  V). c) Output characteristics (film thickness: 281 nm, channel width: 2 mm, channel length: 60  $\mu$ m). d) Transfer characteristics and the transconductance of PEDOT:DNA OEET device ( $g_m = 0.16$  mS for  $V_D = -0.7$  V). e) Output characteristics (film thickness: 263 nm, channel width: 2 mm, channel length: 60  $\mu$ m). f) Transfer characteristics and the transconductance of PPy:DNA-based OEET devices ( $g_m = 0.06$  mS for  $V_D = -0.7$  V). g) Output characteristics (film thickness: 250 nm, channel width: 2 mm, channel length: 60  $\mu$ m).

cellulose dialysis membrane with 12–14 kDa molecular weight cut-off (MWCO) was used to diffuse low molecular weight compounds or residuals in aqueous solution to obtain the final product.

**Material Characterization:** Optical characterization was carried out using PerkinElmer Lambda 1050 UV–vis and FT-Raman microscope RamanScope III from Bruker. For Raman Spectroscopy analysis, the

films are drop-casted on the quartz substrate and excited at 1064 nm. The Raman frequencies are listed below:

PEDOT:PSS (PH 1000): 438  $\text{cm}^{-1}$  (C–O–C deformation), 988  $\text{cm}^{-1}$  (oxyethylene ring deformation), 1257  $\text{cm}^{-1}$  ( $\text{C}_{\alpha}$ – $\text{C}_{\alpha}$  inter-ring stretching), 1367  $\text{cm}^{-1}$  ( $\text{C}_{\beta}$ – $\text{C}_{\beta}$  stretching), 1420  $\text{cm}^{-1}$  ( $\text{C}_{\alpha}$ – $\text{C}_{\beta}$  symmetrical).

PPy: 1379  $\text{cm}^{-1}$  (C=C symmetry stretching), 1490  $\text{cm}^{-1}$ , 1581  $\text{cm}^{-1}$  ( $\text{C}_{\alpha}$ – $\text{C}_{\alpha}$  inter-ring stretching).

DNA: 560  $\text{cm}^{-1}$ , 621  $\text{cm}^{-1}$ , and 710  $\text{cm}^{-1}$  (DNA nucleobases), 789  $\text{cm}^{-1}$  (cytosine, thymine, phosphate bond), 1094  $\text{cm}^{-1}$  (phosphodiester bond).

PEDOT:DNA: 438  $\text{cm}^{-1}$ , 701  $\text{cm}^{-1}$ , 850  $\text{cm}^{-1}$ , 987  $\text{cm}^{-1}$ , 1096  $\text{cm}^{-1}$ , 1259  $\text{cm}^{-1}$ , 1363  $\text{cm}^{-1}$ , 1423  $\text{cm}^{-1}$ .

PPy:DNA: 932  $\text{cm}^{-1}$ , 1072  $\text{cm}^{-1}$ , 1094  $\text{cm}^{-1}$ , 1245  $\text{cm}^{-1}$ , 1378  $\text{cm}^{-1}$ , 1488  $\text{cm}^{-1}$ , 1580  $\text{cm}^{-1}$ .

**Film Characterization:** Glass substrates (150 × 150 mm) were used to obtain spectroscopy and AFM data. ITO-coated glass substrates (130 × 130 mm) were used for SEM measurements. All substrates were cleaned by sonicating in acetone and isopropanol, respectively for 15 min and then blow-dried with nitrogen ( $\text{N}_2$ ). After that, plasma cleaning was used to remove impurities and contaminants from the substrate surface through applying oxygen plasma treatment for 5 min with low RF power of  $\approx 50$  W. The films were subsequently deposited onto clean substrates by drop-casting or spin-coating methods. The dispersed solution of biocomposites (with and without additives) was directly used for film formation. 2.5  $\text{g L}^{-1}$  DNA solution was prepared in water to drop-cast. A KLM spin-coater SCC was utilized for deposition of the thin films. All the films were dried at 140 °C for 1 h. The film thicknesses were determined by using the tactile profilometry setup, a Bruker's DektakXT with a stylus tip radius of 12.5  $\mu\text{m}$ .

SEM images were obtained using SEM ZEISS 1540 XB cross-beam scanning microscope equipped with a focused ion beam unit.

AFM measurements were carried out with the help of the Bruker Innova atomic force microscope.

The electrical sheet resistance of prepared films was measured with Signatone four-point probe station.

**OECT Fabrication:** The OECT devices were fabricated on cleaned glass substrates. Cr/Au with the thickness of 10 nm/100 nm was evaporated at a pressure of  $1 \times 10^{-6}$  mbar through a shadow mask to pattern source and drain electrodes (channel length:  $L = 60 \mu\text{m}$ , channel width  $W = 2 \text{ mm}$ ). The conducting polymers (PEDOT:PSS PH 1000, PEDOT:DNA, and PPy:DNA) were spin-coated on the patterned channel area. The mixture of 94.5% v/v dispersed solutions, 5% v/v glycerol, 0.5% v/v DBSA, and afterward addition of 1% v/v GOPS into the prepared solution was utilized for device fabrication. Subsequently, the spin-coated thin films were annealed at 140 °C for 1 h.

Polydimethylsiloxane (PDMS) well was placed in the middle of the channel area to confine the source and drain electrodes. 20  $\mu\text{L}$  phosphate buffered saline (PBS) solution ( $50 \times 10^{-3} \text{ M}$ ,  $\text{pH} = 7.4$ ) as an electrolyte was filled into the PDMS well and a nonpolarizable gate electrode silver/silver chloride (Ag/AgCl) wire was immersed in the PBS solution.

All the device characterizations were carried out in air using an Agilent model E5273A with a two source-measurement unit instrument which was employed for the steady-state current–voltage measurements.

## Supporting Information

Supporting Information is available from the Wiley Online Library or from the author.

## Acknowledgements

The authors gratefully acknowledge Dr. Christoph Ulbricht for fruitful discussions. This work was financially supported by the European Regional Development Fund (EFRE) within the project “ENZYMBIOKAT”

(GZ2018-98279-2). Financial support of the Austrian Science Foundation (FWF) with the Wittgenstein Prize (Z222 N19) for N.S.S. is gratefully acknowledged.

## Conflict of Interest

The authors declare no conflict of interest.

## Keywords

conductive biocomposites, deoxyribonucleic acid (DNA), materials for bioelectronics, organic electrochemical transistors, PEDOT:DNA, polypyrrole:DNA

Received: August 15, 2019

Revised: October 15, 2019

Published online: November 18, 2019

- [1] N. Claudio, *Molecular Bioelectronics*, World Scientific Publishing Co., Singapore **1996**.
- [2] H. Willner, E. Katz, *Bioelectronics: From Theory to Applications*, Wiley-VCH, Weinheim, Germany **2005**.
- [3] A. Offenhäuser, R. Rinaldi, *Nanobioelectronics – For Electronics, Biology, and Medicine*, Springer, New York **2009**.
- [4] D. A. Bernards, R. M. Owens, G. G. Malliaras, *Organic Semiconductors in Sensor Applications*, Springer, Heidelberg **2010**.
- [5] J. Leger, M. Berggren, S. Carter, *Iontronics*, Taylor & Francis Group, USA **2011**.
- [6] R. Pethig, S. Smith, *Introductory Bioelectronics: For Engineers and Physical Scientists*, Wiley, UK **2013**.
- [7] C. Karunakaran, K. Bhargava, R. Benjamin, *Biosensors and Bioelectronics*, Elsevier, USA **2015**.
- [8] S. Carrara, K. Iniewski, *Handbook of Bioelectronics – Directly Interfacing Electronics and Biological Systems*, Cambridge University Press, UK **2015**.
- [9] N. Claudio, *Molecular Bioelectronics – The 19 Years of Progress*, 2nd ed., World Scientific Publishing Company, Singapore **2016**.
- [10] M. Irimia-Vladu, E. D. Glowacki, N. S. Sariciftci, S. Bauer, *Green Materials for Electronics*, Wiley-VCH, Weinheim, Germany **2018**.
- [11] K. Pal, H.-B. Kraatz, A. Khasnobish, S. Bag, I. Banerjee, U. Kuruganti, *Bioelectronics and Medical Devices*, Woodhead Publishing, UK **2019**.
- [12] O. Parlak, A. Salleo, A. Turner, *Wearable Bioelectronics*, Elsevier, New York **2019**.
- [13] J. M. Leger, *Adv. Mater.* **2008**, *20*, 837.
- [14] G. Tarabella, F. M. Mohammadi, N. Coppede, F. Barbero, S. Iannotta, C. Santato, F. Cicoira, *Chem. Sci.* **2013**, *4*, 1395.
- [15] E. Stavrinidou, P. Leleux, H. Rajaona, D. Khodagholy, J. Rivnay, S. Sanaur, G. G. Malliaras, *Adv. Mater.* **2013**, *25*, 4488.
- [16] M. Wang, G. Mi, D. Shi, N. Bassous, D. Hickey, T. J. Webster, *Adv. Funct. Mater.* **2018**, *28*, 1.
- [17] E. Zeglio, O. Inganäs, *Adv. Mater.* **2018**, *30*, 1800941.
- [18] M. Ecker, A. Joshi-Imre, R. Modi, C. L. Frewin, A. Garcia-Sandoval, J. Maeng, G. Gutierrez-Heredia, J. J. Pancrazio, W. E. Voit, *Multifunct. Mater.* **2018**, *2*, 012001.
- [19] G. W. Omokhunu, C. Bach, *Eur. J. Eng. Res. Sci.* **2019**, *4*, 85.
- [20] E. Zeglio, A. L. Rutz, T. E. Winkler, G. G. Malliaras, A. Herland, *Adv. Mater.* **2019**, *31*, 22.
- [21] H. Shirakawa, J. Louis, A. G. Macdiarmid, *J. Chem. Soc., Chem. Commun.* **1977**, *16*, 578.

- [22] H. S. Nalwa, *Handbook of Organic Conductive Molecules and Polymers*, Vol. 2, Wiley, England **1997**.
- [23] M. Pope, C. E. Swenberg, *Electronic Processes in Organic Crystals and Polymers*, Oxford University Press, New York **1999**.
- [24] G. Hadziioannou, P. F. Van Hutten, *Semiconducting Polymers: Chemistry, Physics, and Engineering*, Wiley-VCH, Weinheim, Germany **2000**.
- [25] M. Schwoerer, H. C. Wolf, *Organic Molecular Solids*, Wiley-VCH, Weinheim, Germany **2007**.
- [26] A. J. Heeger, N. S. Sariciftci, E. B. Namdas, *Semiconducting and Metallic Polymers*, Oxford University Press, New York **2010**.
- [27] E. Noelting, *Scientific and Industrial History of Aniline Black*, Wm. J. Matheson & Co., New York **1889**.
- [28] H. Letheby, *J. Chem. Soc.* **1862**, 15, 161.
- [29] A. G. Green, A. E. Woodhead, *J. Chem. Soc., Trans.* **1910**, 97, 2388.
- [30] A. G. Green, S. Wolff, *Ber. Dtsch. Chem. Ges.* **1911**, 44, 2570.
- [31] A. G. Green, A. E. Woodhead, *J. Chem. Soc., Trans.* **1912**, 101, 1117.
- [32] A. G. Bayer, *European Patent 339 340*, **1988**.
- [33] L. Groenendaal, F. Jonas, D. Freitag, H. Pielartzik, J. R. Reynolds, *Adv. Mater.* **2000**, 12, 481.
- [34] A. Elschner, S. Kirchmeyer, W. Lövenich, U. Merker, K. Reuter, *PEDOT: Principles and Applications of an Intrinsically Conductive Polymer*, Taylor & Francis Group, USA **2011**.
- [35] J. T. Mabeck, J. A. DeFranco, D. A. Bernardis, G. G. Malliaras, *Appl. Phys. Lett.* **2005**, 87, 013503.
- [36] D. Nilsson, N. Robinson, M. Berggren, R. Forchheimer, *Adv. Mater.* **2005**, 17, 353.
- [37] D. Nilsson, M. Chen, T. Kugler, T. Remonen, M. Armgarth, M. Berggren, *Adv. Mater.* **2002**, 14, 51.
- [38] P. O. Svensson, D. Nilsson, R. Forchheimer, M. Berggren, *Appl. Phys. Lett.* **2008**, 93, 203301.
- [39] J. Rivnay, P. Leleux, M. Ferro, M. Sessolo, A. Williamson, D. A. Koutsouras, D. Khodagholy, M. Ramuz, X. Strakosas, R. M. Owens, C. Benar, J.-M. Badier, C. Bernard, G. G. Malliaras, *Sci. Adv.* **2015**, 1, e1400251.
- [40] D. Khodagholy, J. Rivnay, M. Sessolo, M. Gurfinkel, P. Leleux, L. H. Jimison, E. Stavrinidou, T. Herve, S. Sanaur, R. M. Owens, G. G. Malliaras, *Nat. Commun.* **2013**, 4, 2133.
- [41] J. Rivnay, R. M. Owens, G. G. Malliaras, *Chem. Mater.* **2014**, 26, 679.
- [42] Y. Wen, J. Xu, *J. Polym. Sci., Part A: Polym. Chem.* **2017**, 55, 1121.
- [43] H. S. White, G. P. Kittleson, M. S. Wrighton, *J. Am. Chem. Soc.* **1984**, 106, 5375.
- [44] M. J. Panzer, C. R. Newman, C. D. Frisbie, *Appl. Phys. Lett.* **2005**, 86, 10.
- [45] P. Lin, F. Yan, *Adv. Mater.* **2012**, 24, 34.
- [46] J. Isaksson, P. Kjäll, D. Nilsson, N. Robinson, M. Berggren, A. Richter-Dahlfors, *Nat. Mater.* **2007**, 6, 673.
- [47] D. T. Simon, S. Kurup, K. C. Larsson, R. Hori, K. Tybrandt, M. Gojny, E. W. H. Jager, M. Berggren, B. Canlon, A. Richter-Dahlfors, *Nat. Mater.* **2009**, 8, 742.
- [48] J. Liao, H. Si, X. Zhang, S. Lin, *Sensors* **2019**, 19, 218.
- [49] E. W. Paul, A. J. Ricco, M. S. Wrighton, *J. Phys. Chem.* **1985**, 89, 1441.
- [50] V. Rani, K. S. V. Santhanam, *J. Solid State Electrochem.* **1998**, 2, 99.
- [51] J. W. Thackeray, H. S. White, M. S. Wrighton, *J. Phys. Chem.* **1985**, 89, 5133.
- [52] M. Asplund, E. Thaning, J. Lundberg, A. C. Sandberg-Nordqvist, B. Kostyszyn, H. von Holst, *Biomed. Mater.* **2009**, 4, 045009.
- [53] B. Wei, J. Liu, L. Ouyang, C. C. Kuo, D. C. Martin, *ACS Appl. Mater. Interfaces* **2015**, 7, 15388.
- [54] C. Boehler, Z. Aqrave, M. Asplund, *Bioelectron. Med.* **2019**, 2, 89.
- [55] R. X. He, M. Zhang, F. Tan, P. H. M. Leung, X.-Z. Zhao, H. L. W. Chan, M. Yang, F. Yan, *J. Mater. Chem.* **2012**, 22, 22072.
- [56] D. Mantione, I. del Agua, W. Schaafsma, M. ElMahmoudy, I. Uguz, A. Sanchez-Sanchez, H. Sardon, B. Castro, G. G. Malliaras, D. Mecerreyes, *ACS Appl. Mater. Interfaces* **2017**, 9, 18254.
- [57] S. Inal, J. Rivnay, P. Leleux, M. Ferro, M. Ramuz, J. C. Brendel, M. M. Schmidt, M. Thelakkat, G. G. Malliaras, *Adv. Mater.* **2014**, 26, 7450.
- [58] C. B. Nielsen, A. Giovannitti, D.-T. Sbircea, E. Bandiello, M. R. Niazi, D. A. Hanifi, M. Sessolo, A. Amassian, G. G. Malliaras, J. Rivnay, I. McCulloch, *J. Am. Chem. Soc.* **2016**, 138, 10252.
- [59] E. Zeglio, M. Vagin, C. Musumeci, F. N. Aijan, R. Gabrielsson, X. T. Trinh, N. T. Son, A. Maziz, N. Solin, O. Inganäs, *Chem. Mater.* **2015**, 27, 6385.
- [60] L. R. Savagian, A. M. Österholm, J. F. Ponder, K. J. Barth, J. Rivnay, J. R. Reynolds, *Adv. Mater.* **2018**, 30, 1804647.
- [61] A. Giovannitti, I. P. Maria, D. Hanifi, M. J. Donahue, D. Bryant, K. J. Barth, B. E. Makdah, A. Savva, D. Moia, M. Zetek, P. R. F. Barnes, O. G. Reid, S. Inal, G. Rumbles, G. G. Malliaras, J. Nelson, J. Rivnay, I. McCulloch, *Chem. Mater.* **2018**, 30, 2945.
- [62] H. Sun, M. Vagin, S. Wang, X. Crispin, R. Forchheimer, M. Berggren, S. Fabiano, *Adv. Mater.* **2018**, 30, 9.
- [63] M. Moser, J. F. Ponder, A. Wadsworth, A. Giovannitti, I. McCulloch, *Adv. Funct. Mater.* **2019**, 29, 21.
- [64] X. Strakosas, B. Wei, D. C. Martin, R. M. Owens, *J. Mater. Chem. B* **2016**, 4, 4952.
- [65] H. Peng, L. Zhang, C. Soeller, J. Travas-Sejdic, *Biomaterials* **2009**, 30, 2132.
- [66] D. Mantione, I. del Agua, A. Sanchez-Sanchez, D. Mecerreyes, *Polymers* **2017**, 9, 354.
- [67] Y. Ner, M. A. Invernale, J. G. Grote, J. A. Stuart, G. A. Sotzing, *Synth. Met.* **2010**, 160, 351.
- [68] F. Ouchen, P. P. Yaney, C. M. Bartsch, E. M. Heckman, J. G. Grote, *SPIE Proc.* **2010**, 7765, 7765OA.
- [69] L. Wang, J. Yoshida, N. Ogata, S. Sasaki, T. Kajiyama, *Chem. Mater.* **2001**, 13, 1273.
- [70] B. Singh, N. S. Sariciftci, J. G. Grote, F. K. Hopkins, *J. Appl. Phys.* **2006**, 100, 024514.
- [71] P. Stadler, K. Oppelt, T. B. Singh, J. G. Grote, R. Schwödiauer, S. Bauer, H. Piglmayer-Brezina, D. Bauerle, N. S. Sariciftci, *Org. Electron.* **2007**, 8, 648.
- [72] C. Yumusak, T. B. Singh, N. S. Sariciftci, J. G. Grote, *Appl. Phys. Lett.* **2009**, 95, 263304.
- [73] A. J. Steckl, H. Spaeth, H. You, E. Gomez, J. G. Grote, *Opt. Photonics News* **2011**, 22, 34.
- [74] A. Håkansson, S. Han, S. Wang, J. Lu, S. Braun, M. Fahlman, M. Berggren, X. Crispin, S. Fabiano, *J. Polym. Sci., Part B: Polym. Phys.* **2017**, 55, 814.
- [75] L. Kergoat, B. Piro, D. T. Simon, M. C. Pham, V. Noël, M. Berggren, *Adv. Mater.* **2014**, 26, 5658.
- [76] S. Zhang, P. Kumar, A. S. Nouas, L. Fontaine, H. Tang, F. Ciciora, *APL Mater.* **2015**, 3, 1.